

弹性地基上多孔二维功能梯度材料 微梁自由振动研究*

赵英治, 唐怀平, 赖泽东, 章家杰

(西南交通大学 力学与航空航天学院, 成都 610031)

摘要: 基于修正偶应力和 Timoshenko 梁理论, 利用 Hamilton 变分原理推导了 Winkler 弹性地基上多孔二维功能梯度材料 (2D-FGM) 微梁的振动控制方程, 采用微分求积法获得固支-固支 (C-C)、简支-简支 (S-S) 边界条件下微梁的振动频率和基本振型, 对刚度矩阵进行数学处理后极大地提高了计算效率, 将该文模型退化为宏观和微观二维功能梯度模型且与已有文献对比验证其正确性, 算例结果表明: 该文数学模型适用于不同类型的二维材料分布; 微梁的无量纲振动频率随着 Winkler 弹性地基模量的增大而增大; 在一定 Winkler 弹性地基模量下, 微梁的无量纲振动频率随着功能梯度指数、轴向功能梯度指数、孔隙率的增大而减小, 材料变化对振动模态的影响随着振动模态阶数的增加而增加, 同样参数下, 孔隙均匀分布时梁频率略小于孔隙线性分布的情况。

关键词: 修正偶应力理论; 孔隙率; Winkler 弹性地基; 二维功能梯度材料; 微分求积法

中图分类号: O342 **文献标志码:** A **DOI:** 10.21656/1000-0887.440050

Free Vibration Analysis of Porous 2D Functionally Graded Material Microbeams on Winkler's Foundation

ZHAO Yingzhi, TANG Huaiping, LAI Zedong, ZHANG Jiajie

(School of Mechanics and Aerospace Engineering, Southwest Jiaotong University, Chengdu 610031, P.R.China)

Abstract: Based on the modified couple stress theory and the Timoshenko beam theory, the governing equations for free vibration of porous 2D functional graded material (FGM) on Winkler's foundation were derived under Hamilton's principle. The differential quadrature method was used to obtain the numerical solutions of the vibration frequencies and fundamental mode shapes of microbeams with both ends clamped (C-C) and simply supported (S-S). The improved stiffness matrix was used to greatly improve the calculation efficiency. The proposed model was degenerated to the macro and micro 2D-FGM models, which were compared with those in previous literatures for validation. The results show that, the present mathematical model is suitable for different types of 2D material distributions. The dimensionless frequencies increase with the dimensionless elastic modulus of Winkler's foundation. Under a certain dimensionless elastic foundation modulus, the dimensionless frequencies decrease with the functionally graded index, the axial functionally graded index and the porosity.

* 收稿日期: 2023-02-27; 修订日期: 2023-04-03

基金项目: 国家自然科学基金项目 (51778548)

作者简介: 赵英治 (1999—), 男, 硕士生 (E-mail: 964003289@qq.com);

唐怀平 (1967—), 男, 副教授, 博士 (通讯作者, E-mail: thp-vib@163.com).

引用格式: 赵英治, 唐怀平, 赖泽东, 章家杰. 弹性地基上多孔二维功能梯度材料微梁自由振动研究[J]. 应用数学和力学, 2023, 44(11): 1354-1365.

The effect of the material variation on the mode shape increases with the mode number. For the same parameter, the dimensionless frequencies of the beam with uniform porosity distribution are slightly lower than those with linear porosity distribution.

Key words: modified couple stress theory; porosity; Winkler's foundation; 2D functionally graded material; differential quadrature method

0 引 言

功能梯度材料(functionally graded material, FGM)^[1]是一种新型非均质复合材料,常由陶瓷和金属复合而成,内部逐渐改变组成材料的体积分数使得材料性能沿某一方向以连续的方式逐渐变化。FGM 最初应用于航空航天领域,高速飞行使得机身内外存在很大的温差,从而导致材料内部产生热应力,而 FGM 能够将陶瓷的热阻性能和金属的机械性能结合在一起,解决了这一问题。经过数十年的发展,FGM 的应用已经从最初的航空航天工程拓展到了军事、汽车、生物医学、土木工程、制造业和核工业等领域。

在过去几十年中,研究人员利用经典连续介质理论对宏观 FGM 结构的静动态力学行为做了很多研究^[2-10]。如今 FGM 已经应用到到微纳米结构中,例如微电子机械系统(micro electro mechanical system, MEMS)^[11]。微型化是当今科学技术的主要发展方向之一,梁是微电子机械系统中广泛使用的主要结构之一。传统连续介质力学中的本构关系不包括反映构件大小的尺度参数,所以不能预测尺寸效应^[12],针对传统理论的这一缺陷有学者就提出了偶应力理论^[13]和修正偶应力理论^[14]。周强^[15]基于 Timoshenko 梁理论,推导了压电纳米梁的频率方程和振型方程的精确解。Şimşek 等^[16]研究了 FGM 微梁静态弯曲问题,得到受集中荷载和均布荷载简支梁挠度的数值解。Ke 等^[17]基于修正的偶应力理论,利用 Hamilton 原理导出了功能梯度 Timoshenko 微梁的控制方程和边界条件,研究了 FGM 微梁的动力稳定性问题。Şimşek 和 Reddy^[18]结合各种高阶剪切变形理论和修正偶应力理论,研究了 FGM 微梁的静态弯曲和自由振动。考虑物理中面的影响,Al-Basyouni 等^[19]基于修正偶应力理论研究了 FGM 微梁的弯曲和振动特性。Akgöz 等^[20]结合 Euler-Bernoulli 梁理论和修正偶应力理论,研究了变截面轴向 FGM 微梁的自由振动问题。刘松正等^[21]基于四参数高阶剪切-法向伸缩变形理论发展出一种准三维 FGM 微梁模型。结合修正偶应力和 Timoshenko 梁理论,雷剑等^[22]研究了变截面 2D-FGM 微梁的自由振动和屈曲问题。Chen 等^[23]基于高阶剪切变形理论研究了嵌入弹性介质中的 2D-FGM 微梁的自由振动、屈曲和动力稳定性。

起初由于制备工艺存在缺陷,不可避免地导致 FGM 在制备过程中内部产生孔隙,后来人们将孔隙规则排列制成点阵材料(开孔),孔径可逐渐由毫米级减小到微米甚至纳米级。因此,针对多孔 FGM 微梁展开力学特性分析研究具有重要的现实意义。Chen 等^[24]基于 Timoshenko 梁理论,研究了多孔 FGM 梁的弹性屈曲和静态弯曲问题。考虑对称和非对称孔隙度分布,Chen 等^[25]基于 Timoshenko 梁理论研究了多孔 FGM 梁的自由振动和受迫振动行为。Lei 等^[26]研究了具有柔性边界约束的多跨多孔 FGM 梁的动力学行为。王伟斌等^[27]基于 Timoshenko 梁理论研究了多孔 FGM 梁的自由振动问题。

文献[28-29]总结了微分求积法和微分求积单元法的新进展,但目前大多数研究主要集中在宏观多孔功能梯度结构的静动态力学分析,且主要集中在材料性能沿厚度或者轴向某一个方向上连续变化,没有考虑材料性能同时沿厚度和轴向连续变化以及孔隙线性分布对功能梯度结构动力特性的影响。本文结合修正偶应力理论和 Timoshenko 梁理论,利用 Hamilton 原理导出弹性地基多孔 2D-FGM 微梁的振动控制方程,统一编写 MATLAB 程序得到了微梁的自振频率和前三阶振型,采用变化后的刚度矩阵极大地提高了微分求积法的计算效率,并将本文模型退化为宏观功能梯度模型和微观均质模型,与已有文献对比验证了其正确性。分析了 Winkler 弹性地基模量、功能梯度指数、孔隙率、孔隙分布模式和梁跨厚比对微梁自由振动的影响。

1 理论模型

1.1 多孔 FGM 微梁

建立如图 1 所示的 Winkler 弹性地基上长度为 L 、厚度为 h 、宽为 b 、多孔二维功能梯度矩形截面梁研究

模型.图中 k_w 为 Winkler 弹性地基模量.梁由陶瓷和金属的混合物制成,梁的材料性能不仅在厚度方向上呈幂函数变化,而且沿梁的轴向(梁的长度方向)也呈幂函数变化,孔隙沿厚度方向呈均匀或线性分布(孔隙分布模式如图 2 所示),使得材料属性均为坐标 x, z 的函数.

多孔 FGM 梁的物性参数,包括弹性模量 $E(x, z, \theta)$ 、密度 $\rho(x, z, \theta)$, 表示为:

孔隙均匀分布

$$p(x, z, \theta) = p_m + (p_c - p_m) \left(\frac{1}{2} + \frac{z}{h} \right)^{P_z} \left(\frac{x}{L} \right)^{P_x} - \frac{\theta}{2}(p_c + p_m); \tag{1}$$

孔隙线性分布

$$p(x, z, \theta) = p_m + (p_c - p_m) \left(\frac{1}{2} + \frac{z}{h} \right)^{P_z} \left(\frac{x}{L} \right)^{P_x} - \frac{\theta}{2}(p_c + p_m) \left(1 - \frac{2|z|}{h} \right), \tag{2}$$

其中, P_z 为梯度指数, P_x 为轴向功能梯度指数,下标 c、m 分别表示陶瓷和金属材料, θ 为孔隙率.

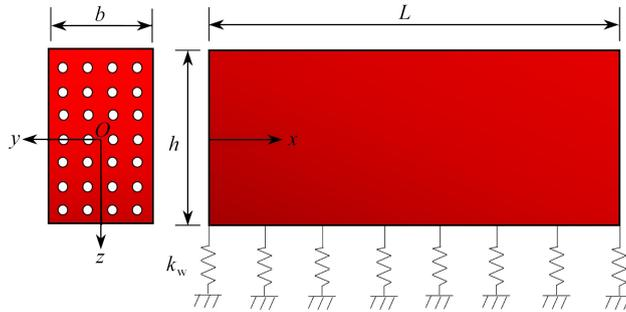
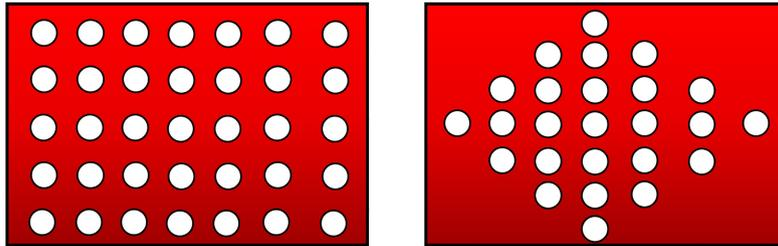


图 1 Winkler 弹性地基上多孔 2D-FGM 微梁几何尺寸及坐标系

Fig. 1 The geometry and coordinates of a porous 2D functionally graded microbeam on Winkler's foundation



(a) 孔隙均匀分布 (b) 孔隙线性分布
(a) The uniform porosity distribution (b) The linear porosity distribution

图 2 孔隙分布模式

Fig. 2 Porosity distribution patterns

1.2 微梁的振动控制方程

使用图 1 所示的直角坐标系 (x, y, z) , Timoshenko 梁的位移场可以表示为

$$\begin{cases} u_1 = U(x, t) + z\Phi(x, t), \\ u_2 = 0, \\ u_3 = W(x, t), \end{cases} \tag{3}$$

其中, u_1, u_2 和 u_3 为梁截面上任一点分别在 x, y, z 方向上的位移分量, Φ 为截面关于垂直方向的转角.

传统连续介质力学理论下,梁的几何方程和物理方程为

$$\varepsilon_{xx} = \frac{\partial U}{\partial x} + z \frac{\partial \Phi}{\partial x}, \quad \varepsilon_{xz} = \frac{1}{2} \left(\frac{\partial W}{\partial x} - \Phi \right), \tag{4}$$

$$\sigma_{xx} = E(x, z, \theta) \left(\frac{\partial U}{\partial x} + z \frac{\partial \Phi}{\partial x} \right), \quad \sigma_{xz} = \kappa \mu(x, z, \theta) \left(\Phi + \frac{\partial W}{\partial x} \right), \tag{5}$$

式中, κ 为剪切修正系数, μ 为剪切模量.

根据 Yang 等^[14]提出的修正偶应力理论,各向同性弹性体本构关系中对称弯曲张量 χ_{ij} 和偶应力张量偏斜部分 m_{ij} 为

$$\chi_{ij} = \frac{1}{2}(e_{ipq}\partial_p\varepsilon_{qj} + e_{ipq}\partial_p\varepsilon_{qi}), \quad (6)$$

$$m_{ij} = 2l^2\mu\chi_{ij}, \quad (7)$$

式中, l 是材料特征长度.

根据式(4)和(6),可得非零曲率分量 χ_{xy} 为

$$\chi_{xy} = \frac{1}{4}\left(\frac{\partial\Phi}{\partial x} - \frac{\partial^2 W}{\partial x^2}\right). \quad (8)$$

将式(8)代入式(7),可得非零偶应力分量 m_{xy} 为

$$m_{xy} = \frac{1}{2}l^2\mu\left(\frac{\partial\Phi}{\partial x} - \frac{\partial^2 W}{\partial x^2}\right), \quad (9)$$

应变能的变分为

$$\delta U = \int_0^L \int_A (\sigma_{ij}\delta\varepsilon_{ij} + m_{ij}\delta\chi_{ij}) dAdx, \quad (10)$$

其中, A 是梁的横截面积.

动能变分为

$$\delta K = \int_0^L \int_A \left\{ \rho(x,z,\theta) \left[\left(\frac{\partial u_1}{\partial t}\right)^2 + \left(\frac{\partial u_2}{\partial t}\right)^2 + \left(\frac{\partial u_3}{\partial t}\right)^2 \right] \right\} dAdx. \quad (11)$$

弹性地基势能在时间间隔 $[0, T]$ 上的一阶变分为

$$\delta V = \int_0^T \int_{\Omega} k_w \delta w dv dt. \quad (12)$$

使用 Hamilton 原理:

$$\delta \int_0^T (K - U - V) dt = 0. \quad (13)$$

惯性系数和弹性系数分别定义为

$$\{A_{11}(x), B_{11}(x), D_{11}(x)\} = \int_A \frac{(1-\nu)E(x,z,\theta)}{(1+\nu)(1-2\nu)} \{1, z, z^2\} dA, \quad (14)$$

$$D_{55}(x) = \int_A \frac{E(x,z,\theta)}{2(1+\nu)} dA, \quad (15)$$

$$\{I_1(x), I_2(x), I_3(x)\} = \int_A \rho(x,z,\theta) \{1, z, z^2\} dA, \quad (16)$$

式中, ν 为材料 Poisson 比.

使用分离变量法对方程进行处理,令

$$\{\Phi(x,t), U(x,t), W(x,t)\} = \{\phi(x), u(x), w(x)\} e^{i\omega_n t}, \quad (17)$$

式中, w_n 为梁频率, i 为虚数单位.

将式(10)–(12)代入式(13)中,得到控制方程:

$$\delta u = 0: \frac{\partial}{\partial x} \left[A_{11}(x) \frac{\partial U}{\partial x} + B_{11}(x) \frac{\partial \Phi}{\partial x} \right] = I_1 w_n^2 u + I_2 w_n^2 \phi, \quad (18)$$

$$\delta w = 0: \frac{\partial}{\partial x} \left[\kappa A_{55}(x) \left(\frac{\partial W}{\partial x} + \Phi \right) \right] + \frac{1}{2} \frac{\partial^2}{\partial x^2} \left[\frac{1}{2} l^2 A_{55}(x) \left(\frac{\partial \Phi}{\partial x} - \frac{\partial^2 W}{\partial x^2} \right) \right] - k_w w = I_1(x) w_n^2 w, \quad (19)$$

$$\delta \phi = 0: \frac{\partial}{\partial x} \left[B_{11}(x) \frac{\partial U}{\partial x} + D_{11}(x) \frac{\partial \Phi}{\partial x} \right] - \kappa A_{55}(x) \left(\frac{\partial W}{\partial x} + \Phi \right) + \frac{1}{2} \frac{\partial}{\partial x} \left[\frac{1}{2} l^2 A_{55}(x) \left(\frac{\partial \Phi}{\partial x} - \frac{\partial^2 W}{\partial x^2} \right) \right] = I_2(x) w_n^2 u + I_3(x) w_n^2 \phi, \quad (20)$$

式中矩形截面梁的 $\kappa = 5/6$.

对于固支-固支(C-C)边界条件应满足

$$u = w = \phi = \frac{\partial w}{\partial x} = 0, \quad \text{at } x = 0 \text{ or } x = L. \quad (21)$$

对于简支-简支(S-S)边界条件应满足

$$\frac{\partial u}{\partial x} = w = \frac{\partial \phi}{\partial x} = \frac{\partial^2 w}{\partial x^2} = 0, \quad \text{at } x = 0 \text{ or } x = L. \quad (22)$$

2 微分求积法(DQM)

微分求积法常用于求解控制方程,不同于往常直接求解刚度矩阵行列式的方法,本文通过对刚度矩阵进行数学处理,求解处理后刚度矩阵特征值的方法来得到梁的振动频率.算例表明,两种方法取的节点数相同时,本文方法所需的时间仅为往常方法的3.64%,且还可以求解梁的模式.

根据微分求积法的离散化法则,位移分量 u, w 和 ϕ 及其相对于 x 的 k 阶导数近似为

$$\{u, w, \phi\} = \sum_{m=1}^N l_m(x) \{u_m, w_m, \phi_m\}, \quad (23)$$

$$\frac{\partial^k}{\partial x^k} \{u, w, \phi\} \Big|_{x=x_i} = \sum_{m=1}^N C_{im}^{(k)} \{u_m, w_m, \phi_m\}, \quad (24)$$

其中 $u_m = u(x_m, t)$, $w_m = w(x_m, t)$, $\phi_m = \phi(x_m, t)$, N 是沿 x 轴分布的节点总数, $l_m(x)$ 是 Lagrange 插值多项式, $C_{im}^{(k)}$ 是权系数.

边界条件的代入选择 δ 法, δ 的取值范围^[30] 为 $10^{-6} \leq \delta \leq 10^{-4}$, δ 过大过小都会造成结果的不收敛,节点的选取如下:

$$\begin{cases} x_1 = 0, x_2 = 0.000 \ 1L, x_{N-1} = 0.999 \ 9L, x_N = L, \\ x_i = \frac{1}{2} \left[1 - \cos \left(\frac{i-2}{N-3} \pi \right) \right] L, \quad i = 3, 4, \dots, N-2. \end{cases} \quad (25)$$

离散后的控制方程为

$$\begin{aligned} & \frac{\partial [A_{11}(x)]}{\partial x} \sum_{m=1}^N C_{im}^{(1)} u_m + A_{11}(x) \sum_{m=1}^N C_{im}^{(2)} u_m + \frac{\partial [B_{11}(x)]}{\partial x} \sum_{m=1}^N C_{im}^{(1)} \phi_m + B_{11}(x) \sum_{m=1}^N C_{im}^{(2)} \phi_m = \\ & - I_1(x) w_n^2 u_i - I_2(x) w_n^2 \phi_i, \end{aligned} \quad (26)$$

$$\begin{aligned} & \frac{\partial [\kappa A_{55}(x)]}{\partial x} \left(\sum_{m=1}^N C_{im}^{(1)} w_m + \phi_i \right) + \kappa A_{55}(x) \left(\sum_{m=1}^N C_{im}^{(1)} \phi_m + \sum_{m=1}^N C_{im}^{(2)} w_m \right) + \\ & \frac{1}{4} l^2 \frac{\partial^2 [\kappa A_{55}(x)]}{\partial x^2} \left(\sum_{m=1}^N C_{im}^{(1)} \phi_m - \sum_{m=1}^N C_{im}^{(2)} w_m \right) + \\ & \frac{1}{2} l^2 \kappa A_{55}(x) \left(\sum_{m=1}^N C_{im}^{(2)} \phi_m - \sum_{m=1}^N C_{im}^{(3)} w_m \right) + \frac{1}{4} l^2 \kappa A_{55}(x) \left(\sum_{m=1}^N C_{im}^{(3)} \phi_m - \sum_{m=1}^N C_{im}^{(4)} w_m \right) - k_w w_i = \\ & - I_1(x) w_n^2 w_i, \end{aligned} \quad (27)$$

$$\begin{aligned} & \frac{\partial [B_{11}(x)]}{\partial x} \sum_{m=1}^N C_{im}^{(1)} u_m + B_{11}(x) \sum_{m=1}^N C_{im}^{(2)} u_m + \frac{\partial [D_{11}(x)]}{\partial x} \sum_{m=1}^N C_{im}^{(1)} \phi_m + \\ & D_{11}(x) \sum_{m=1}^N C_{im}^{(2)} \phi_m - \kappa A_{55}(x) \left(\phi_i + \sum_{m=1}^N C_{im}^{(1)} w_m \right) + \\ & \frac{1}{4} l^2 A_{55}(x) \left(\sum_{m=1}^N C_{im}^{(2)} \phi_m - \sum_{m=1}^N C_{im}^{(3)} w_m \right) + \frac{1}{4} l^2 \frac{\partial [A_{55}(x)]}{\partial x} \left(\sum_{m=1}^N C_{im}^{(1)} \phi_m - \sum_{m=1}^N C_{im}^{(2)} w_m \right) = \\ & - I_2(x) w_n^2 u_i - I_3(x) w_n^2 \phi_i. \end{aligned} \quad (28)$$

对 C-C 边界条件运用微分求积法进行离散:

$x = 0$ 处

$$u_1 = 0, w_1 = 0, \sum_{m=1}^N C_{2m}^{(1)} w_m = 0, \phi_1 = 0;$$

$x = L$ 处

$$u_N = 0, w_N = 0, \sum_{m=1}^N C_{(N-1)m}^{(1)} w_m = 0, \phi_N = 0.$$

对 S-S 边界条件运用微分求积法进行离散:

$x = 0$ 处

$$\sum_{m=1}^N C_{1m}^{(1)} u_m = 0, w_1 = 0, \sum_{m=1}^N C_{2m}^{(2)} w_m = 0, \sum_{m=1}^N C_{1m}^{(1)} \phi_m = 0;$$

$x = L$ 处

$$\sum_{m=1}^N C_{Nm}^{(1)} u_m = 0, w_N = 0, \sum_{m=1}^N C_{(N-1)m}^{(2)} w_m = 0, \sum_{m=1}^N C_{Nm}^{(1)} \phi_m = 0.$$

将式(26)–(28)微梁的振动控制方程转化为向量形式:

$$(\mathbf{K}_1 - w_n^2 \mathbf{M}) \mathbf{X} = \mathbf{0}, \quad (29)$$

式中,系数矩阵 \mathbf{K}_1, \mathbf{M} 分别为刚度矩阵和质量矩阵, \mathbf{K}_1, \mathbf{M} 为 $3N \times 3N$ 的矩阵, \mathbf{X} 是位移分量向量:

$$\mathbf{X} = \{u_1, u_N, w_1, w_2, w_{N-1}, w_N, \phi_1, \phi_N, u_2, \dots, u_{N-1}, w_3, \dots, w_{N-2}, \phi_2, \dots, \phi_{N-1}\}^T. \quad (30)$$

式(29)可以转化为

$$(\mathbf{K}_2 - w_n^2 \mathbf{I}) \mathbf{X} = \mathbf{0}, \quad (31)$$

其中 \mathbf{I} 为单位矩阵,

$$\mathbf{K}_2 = \mathbf{M}^{-1} \mathbf{K}_1. \quad (32)$$

将边界条件代入式(31)得到

$$\mathbf{K} \{u_1, u_N, w_1, w_2, w_{N-1}, w_N, \phi_1, \phi_N, u_2, \dots, u_{N-1}, w_3, \dots, w_{N-2}, \phi_2, \dots, \phi_{N-1}\}^T = w_n^2 \mathbf{I} \{0, 0, 0, 0, 0, 0, 0, 0, u_2, \dots, u_{N-1}, w_3, \dots, w_{N-2}, \phi_2, \dots, \phi_{N-1}\}^T. \quad (33)$$

式(31)的矩阵形式为

$$\mathbf{S}_{bb} \mathbf{X}_b + \mathbf{S}_{bd} \mathbf{X}_d = \mathbf{0}, \quad (34a)$$

$$\mathbf{S}_{db} \mathbf{X}_b + \mathbf{S}_{dd} \mathbf{X}_d = w_n^2 \mathbf{X}_d. \quad (34b)$$

由式(34a)可以得到

$$\mathbf{X}_b = -\mathbf{S}_{bb}^{-1} \mathbf{S}_{bd} \mathbf{X}_d. \quad (35)$$

将式(35)代入式(34b)得

$$\mathbf{S} \mathbf{X}_d - w_n^2 \mathbf{I} \mathbf{X}_d = \mathbf{0}, \quad (36)$$

其中 \mathbf{S} 为 $(3N - 8) \times (3N - 8)$ 的矩阵,

$$\mathbf{S} = -\mathbf{S}_{db} \mathbf{S}_{bb}^{-1} \mathbf{S}_{bd} + \mathbf{S}_{dd}. \quad (37)$$

矩阵 \mathbf{S} 的特征值和特征向量分别为梁的振动频率的平方和振型。

3 算例分析与结果讨论

本节将基于微分求积法,结合若干算例验证本节解的正确性,详细分析无量纲弹性地基模量、功能梯度指数、轴向功能梯度指数、孔隙率、跨厚比等参数对弹性地基多孔 2D-FGM 微梁自由振动的影响。

3.1 结果验证

本小节介绍了数值解的收敛性和精度。数值解的精确性取决于微分求积法插值点的数量,表 1 给出了不同插值点数量下弹性地基多孔 2D-FGM 简支微梁的前三阶无量纲频率,可以看出微梁的前三阶无量纲频率随着 N 的增大而减小。 N 的增加可以减小数值结果的差异,表明微分求积法得到的前三阶无量纲频率收敛。为了提高计算效率,后续研究中采用 $N = 15$, 以确保计算结果的收敛性。

材料物性参数取 $E_m = 70 \text{ GPa}$, $E_c = 380 \text{ GPa}$, $\rho_m = 2700 \text{ kg/m}^3$, $\rho_c = 3800 \text{ kg/m}^3$, 材料特征长度为 $l =$

17.6 μm , 陶瓷和金属材料的 Poisson 比相当接近, 将 Poisson 比假设为常数 $\nu = 0.3$. 为方便与其他文献进行对比, 引入无量纲振动频率 $\Omega_n = \frac{w_n L^2}{h} \sqrt{\frac{\rho_m}{E_m}}$ 和无量纲弹性地基模量 $\lambda = \frac{k_m L^4}{E_m h^3}$.

表1 弹性地基多孔 2D-FGM 微梁无量纲频率收敛性分析

(S-S 边界, $P_x = 1, P_z = 1, \theta = 0.1, L/h = 5, h = 2l, \lambda = 3 \times 10^{-6}$)

Table 1 Convergence verification of dimensionless frequencies of the porous 2D-FGM microbeam on Winkler's foundation

(S-S boundary condition, $P_x = 1, P_z = 1, \theta = 0.1, L/h = 5, h = 2l, \lambda = 3 \times 10^{-6}$)

	N							
	7	9	11	13	15	17	19	21
Ω_1	5.429 7	5.428 5	5.428 3	5.428 3	5.428 3	5.428 3	5.428 3	5.428 3
Ω_2	19.390 2	18.200 1	18.193 4	18.193 2	18.193 2	18.193 2	18.193 2	18.193 2
Ω_3	38.905 4	35.116 2	34.682 9	34.672 5	34.672 4	34.672 4	34.672 4	34.672 4

当无量纲弹性地基模量 λ 和孔隙率 θ 为零时, 本文模型退化为 2D-FGM 微梁模型, 表 2 给出了 C-C 边界条件下 2D-FGM 微梁的一阶无量纲频率并与文献[22]的结果进行对比, 两者数据基本一致, 最大误差不超过 1%, 证明了微分求积法对于本文研究的有效性和正确性。

表 3 给出了 C-C 边界条件下宏观 2D-FGM 梁的一阶无量纲频率与文献[31]中精确解的对比, 两者结果基本一致, 最大误差在 0.5% 以内, 进一步证明了本文数学模型适用于不同类型的二维材料分布. 为了进行比较, 物性参数和几何参数取 $E_{\text{fb}} = 71 \text{ GPa}$, $\rho_{\text{fb}} = 2780 \text{ kg/m}^3$, $\nu = 0.3, h = 0.05 \text{ m}, L = 5 \text{ m}$, 材料特性沿轴向和厚度方向服从指数分布:

$$P(x, z) = P_{\text{fb}} e^{P_z(1/2+z/h) + P_x(x/L)}. \quad (38)$$

表2 C-C 边界条件下 2D-FGM 微梁一阶振动频率

Table 2 Dimensionless frequencies of the 2D functionally graded microbeam under the C-C boundary condition

model	$P_z = 0, P_x = 0$	$P_z = 1, P_x = 0$	$P_z = 0, P_x = 1$	$P_z = 1, P_x = 1$
this paper	28.585 4	23.883 1	22.223 6	19.534 0
ref. [22]	28.577 9	23.677 7	22.427 6	19.546 4

表3 基于本文模型的宏观 2D-FGM 梁无量纲频率与文献中结果的对比(C-C 边界)

Table 3 Comparison of the dimensionless fundamental frequencies of the C-C bi-directional functionally graded beam

model		$P_z = 0$	$P_z = 2$	$P_z = 4$	$P_z = 6$	$P_z = 8$
$P_x = 0$	ref. [31]	6.454 1	5.872 9	4.664 3	3.557 0	2.766 1
	this papaer	6.455 2	5.873 7	4.664 7	3.557 1	2.766 1
$P_x = 2$	ref. [31]	6.616 8	6.021 0	4.782 0	3.646 7	2.835 9
	this papaer	6.617 9	6.021 8	4.782 3	3.646 9	2.835 9
$P_x = 4$	ref. [31]	7.150 6	6.506 8	5.167 9	3.941 1	3.064 8
	this papaer	7.152 3	6.508 1	5.168 6	3.941 4	3.065 0
$P_x = 6$	ref. [31]	8.162 0	7.427 3	5.899 0	4.498 7	3.498 5
	this papaer	8.168 3	7.432 7	5.903 0	4.501 6	3.500 6
$P_x = 8$	ref. [31]	9.753 2	8.875 3	7.049 3	5.376 1	4.180 8
	this papaer	9.802 4	8.919 9	7.084 5	5.402 8	4.201 5

3.2 结果分析

表 4 给出了当功能梯度指数 $P_x = 1, P_z = 1$, 跨厚比 $L/h = 5$, 梁截面高度与材料特征长度比值 $h/l = 2$, 孔隙率 $\theta = 0.1$ 时, 无量纲弹性地基模量 λ 对弹性地基上多孔 FGM 微梁前三阶无量纲频率的影响. 可以看出, 微梁的无量纲频率随着无量纲弹性地基模量的增大而增大, 且一阶无量纲频率增加的幅度要大于二阶、三阶。

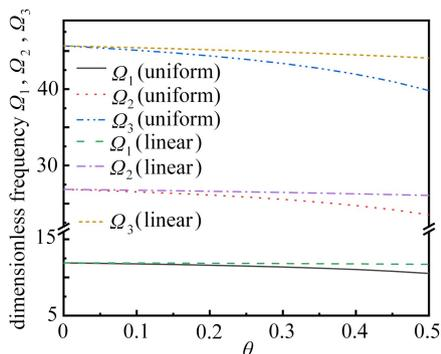
图 3 给出了孔隙均匀分布和线性分布时弹性地基上多孔 2D-FGM 微梁的前三阶无量纲频率与孔隙率 θ 之间的关系曲线. 可以看出, 微梁的前三阶无量纲频率随着孔隙率的增加而减小, 且二阶、三阶减小的幅度大于一阶, 这与弹性地基模量对微梁频率的影响恰恰相反. 同样参数下, 孔隙均匀分布时微梁的频率略小于孔

隙线性分布的情况,这与实际情况相符,因为孔隙均匀分布时孔隙较多,导致梁结构刚度降低得多,此外孔隙率越大,两者的差距越明显。

表 4 无量纲弹性地基模量对前三阶无量纲频率的影响 ($P_x = 1, P_z = 1, \theta = 0.1, L/h = 5, h = 2l$, 孔隙均匀分布)

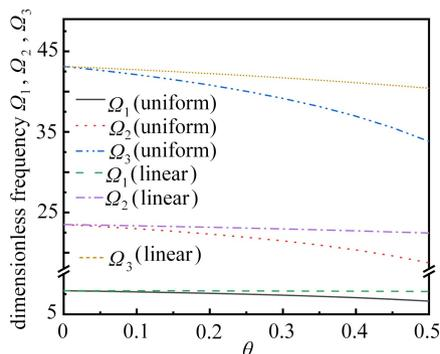
Table 4 Effects of the dimensionless elastic foundation modulus on the 1st 3 orders of dimensionless frequencies ($P_x = 1, P_z = 1, \theta = 0.1, L/h = 5, h = 2l$, uniform porosity distribution)

λ	C-C			S-S		
	Ω_1	Ω_2	Ω_3	Ω_1	Ω_2	Ω_3
0	10.2652	23.536 3	40.299 4	5.581 7	18.666 0	35.487 9
1×10^{-5}	10.272 0	23.539 2	40.301 1	5.593 5	18.669 5	35.489 8
2×10^{-5}	10.278 7	23.542 2	40.302 8	5.605 3	18.673 0	35.491 6
3×10^{-5}	10.285 5	23.545 1	40.304 4	5.617 2	18.676 5	35.493 5
4×10^{-5}	10.292 2	23.548 0	40.306 1	5.628 9	18.680 0	35.495 3
5×10^{-5}	10.299 0	23.550 9	40.307 8	5.640 7	18.683 5	35.497 2
6×10^{-5}	10.305 7	23.553 8	40.309 5	5.652 4	18.687 0	35.499 1
7×10^{-5}	10.312 4	23.556 7	40.311 2	5.664 1	18.690 5	35.500 9
8×10^{-5}	10.319 2	23.559 6	40.312 9	5.675 8	18.694 0	35.502 8
9×10^{-5}	10.325 9	23.562 5	40.314 6	5.687 5	18.697 5	35.504 6
1×10^{-4}	10.332 6	23.565 5	40.316 3	5.699 1	18.701 0	35.506 5



(a) C-C 边界

(a) The C-C boundary condition

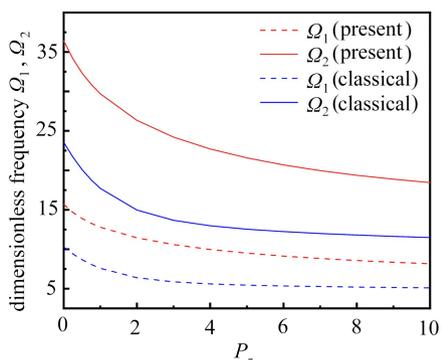


(b) S-S 边界

(b) The S-S boundary condition

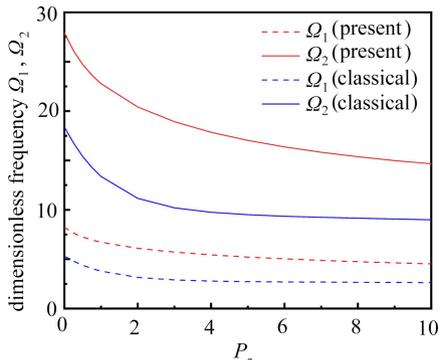
图 3 孔隙率对前三阶无量纲频率的影响 ($P_z = 2, L/h = 5, \lambda = 3 \times 10^{-6}$)

Fig. 3 Effects of the porosity on the 1st 3 dimensionless frequencies ($P_z = 2, L/h = 5, \lambda = 3 \times 10^{-6}$)



(a) C-C 边界

(a) The C-C boundary condition



(b) S-S 边界

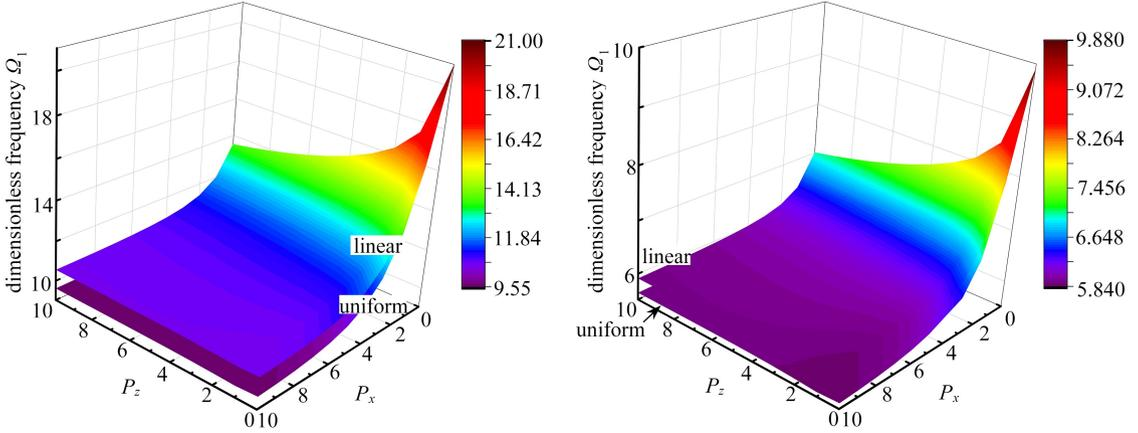
(b) The S-S boundary condition

图 4 不同理论下功能梯度指数对前两阶无量纲频率的影响 ($b = 2h, L = 5h, \theta = 0.2, \lambda = 3 \times 10^{-6}$)

Fig. 4 Effects of the functionally graded index on the 1st 2 dimensionless frequencies under different theories ($b = 2h, L = 5h, \theta = 0.2, \lambda = 3 \times 10^{-6}$)

为了探究功能梯度指数 P_z 对不同理论下梁振动频率的影响,图4给出了 C-C 和 S-S 边界条件下孔隙均匀、线性分布时经典与修正偶应力理论下功能梯度指数 P_z 与弹性地基多孔 FGM 梁的前二阶无量纲频率的关系曲线.可以看出,相较于经典理论,修正偶应力理论下的梁频率更高,但无论哪种理论下,微梁的无量纲频率均随着功能梯度指数 P_z 的增大而减小,且二阶无量纲频率随功能梯度指数增加而减小的幅度要大于一阶频率.

为了探究不同方向功能梯度指数对梁振动频率的影响,图5分别给出了 C-C、S-S 边界条件下功能梯度指数 P_z 和 P_x 共同对弹性地基多孔 2D-FGM 微梁一阶无量纲频率的影响曲面.可以看出当功能梯度指数较小时 ($P_z \leq 2, P_x \leq 2$), 梁无量纲频率随着功能梯度指数的增加迅速减小,之后随着功能梯度指数的进一步增加,频率减小的趋势趋于平缓.此外,轴向功能梯度指数 P_x 对微梁频率的影响更明显.



(a) C-C 边界

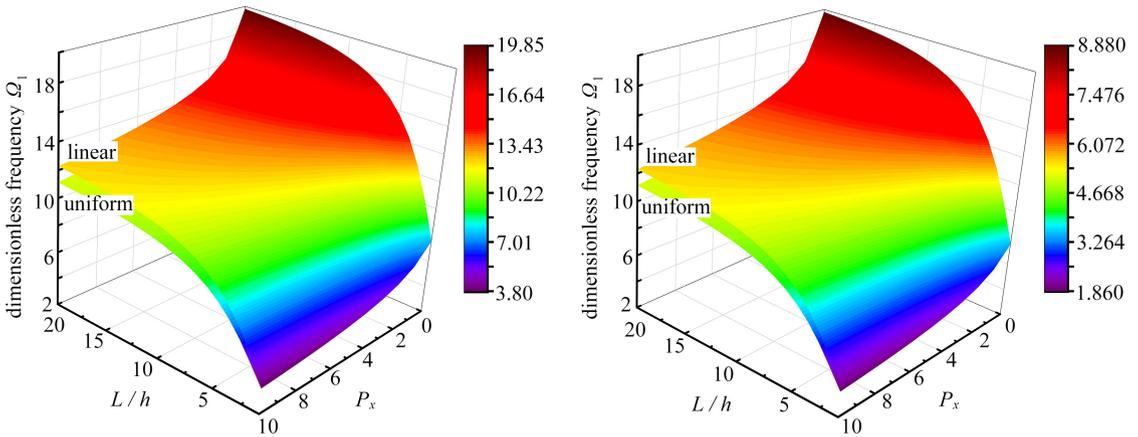
(a) The C-C boundary condition

(b) S-S 边界

(b) The S-S boundary condition

图5 功能梯度指数 P_z 和 P_x 共同对弹性地基多孔 2D-FGM 微梁一阶无量纲频率的影响 ($\theta = 0.2, \lambda = 3 \times 10^{-6}$)

Fig. 5 The effects of P_z and P_x on the dimensionless fundamental frequency of porous 2D-FGM microbeams ($\theta = 0.2, \lambda = 3 \times 10^{-6}$)



(a) C-C 边界

(a) The C-C boundary condition

(b) S-S 边界

(b) The S-S boundary condition

图6 跨厚比和功能梯度指数共同对弹性地基多孔 2D-FGM 梁一阶无量纲频率的影响 (孔隙均匀分布, $\theta = 0.2, \lambda = 3 \times 10^{-6}$)

Fig. 6 The effects of the span-to-depth ratio and the functionally graded index on the dimensionless fundamental frequencies of porous 2D-FGM microbeams (uniform porosity distribution, $\theta = 0.2, \lambda = 3 \times 10^{-6}$)

图6给出了 C-C 和 S-S 边界条件下跨厚比 L/h 和功能梯度指数 P_z 共同对弹性地基多孔 2D-FGM 微梁一阶无量纲频率的影响曲面.可以看出:微梁的一阶无量纲频率随着 L/h 的增加而增加,当 L/h 较小时 ($L/h < 6$), 频率增加幅度非常明显;但当跨厚比进一步增大时,跨厚比对微梁频率的影响不明显.同样条件下,功能

梯度指数对不同跨厚比的微梁频率的影响基本一致。

图 7 和图 8 分别给出了 C-C、S-S 边界条件下弹性地基多孔 2D-FGM 微梁的前三阶振动模态。可以看出: 当梁为均质材料时 ($P_x = 0, P_z = 0$), 梁的振动模态关于梁中点对称或反对称, 最大模态位移位于跨中; 但是当材料沿轴向或厚度方向变化时, 梁的振动模态不再关于梁中点对称或反对称, 最大模态位移也偏离跨中; 一阶振动模态受材料变化影响最小, 随着振动模态阶数的增加, 材料变化对振动模态影响增加。此外, 材料变化对 C-C 梁振动模态的影响比 S-S 梁明显。为了使微分求积法得到的梁振动模态足够光滑, N 取 71, w_{\max} 为 4 个模态位移列向量中绝对值的最大值。

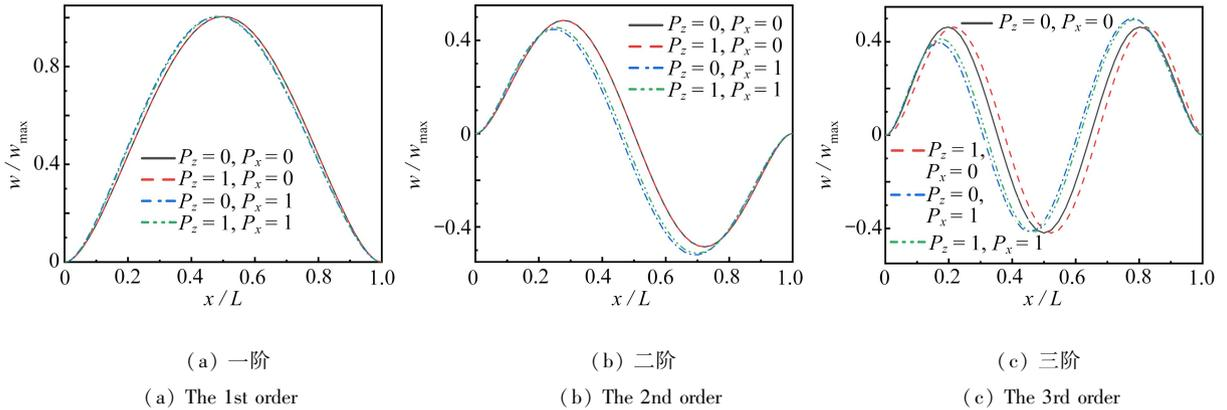


图 7 弹性地基上多孔 2D-FGM 微梁的前三阶振动模态 (C-C 边界)

Fig. 7 The 1st 3 mode shape of the porous 2D-FGM microbeam on Winkler's foundation (C-C boundary condition)

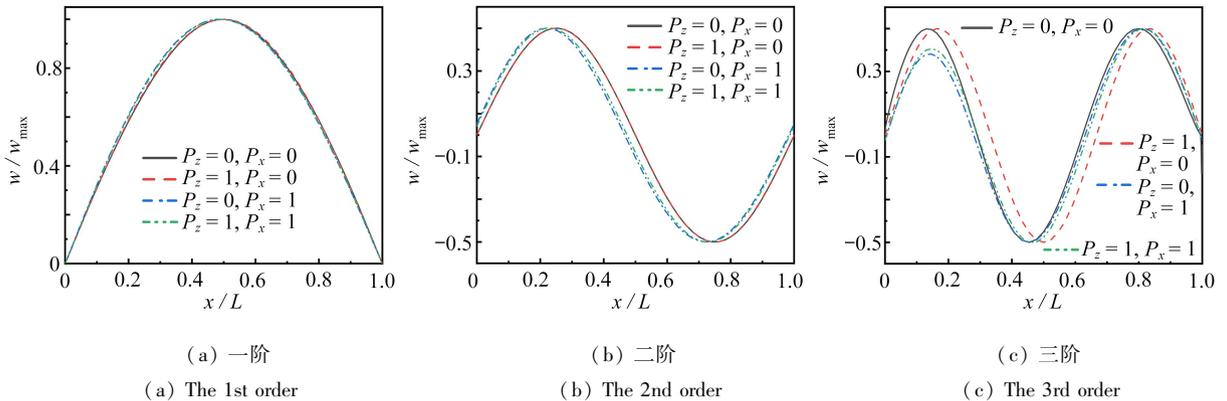


图 8 弹性地基上多孔 2D-FGM 微梁的前三阶振动模态 (S-S 边界)

Fig. 8 The 1st 3 mode shapes of the porous 2D-FGM microbeam on Winkler's foundation (S-S boundary condition)

4 结 论

本文基于修正偶应力理论和 Timoshenko 梁理论, 利用微分求积法求解得到了 Winkler 弹性地基上多孔 2D-FGM 微梁自振问题数值解。结果表明:

1) 本文采用处理后的刚度矩阵, 极大地提高了微分求积法的计算效率, 统一编写 MATLAB 程序与已有文献进行退化验证, 两者结果非常接近, 说明了本文模型适用于不同类型的二维材料分布以及该分析方法对修正偶应力理论下梁自由振动问题的可行性。

2) 微梁的振动频率均随着梯度指数、孔隙率的增加而减小, 随着 Winkler 弹性地基模量的增加而增大, 孔隙率、功能梯度指数的改变对低阶频率影响小, 地基弹性模量的改变对高阶频率影响小, 同样条件下孔隙均匀分布的微梁频率略小于孔隙线性分布的微梁。

3) 当跨厚比 L/h 较小时 ($L/h < 6$), 微梁频率随 L/h 增大而增大的幅度明显, 但当跨厚进一步增大时, 跨厚比对微梁频率的影响则不明显。

4) 材料变化使得梁的一阶振动模态不再关于跨中对称,最大模态位移也偏离跨中,材料沿轴向变化时这一现象较明显.材料变化对一阶振动模态的影响最小,随着振动模态阶数的增加对振动模态的影响也越大。

参考文献(References):

- [1] UDUPA G, RAO S S, GANGADHARAN K V. Functionally graded composite materials: an overview[J]. *Procedia Materials Science*, 2014, **5**: 1291-1299.
- [2] SANKAR B V. An elasticity solution for functionally graded beams[J]. *Composites Science and Technology*, 2001, **61**(5): 689-696.
- [3] MALEKZADEH P, KARAMI G, FARID M. DQEM for free vibration analysis of Timoshenko beams on elastic foundations[J]. *Computational Mechanics*, 2003, **31**(3/4): 219-228.
- [4] SHARIAT B A S, ESLAMI M R. Buckling of thick functionally graded plates under mechanical and thermal loads[J]. *Composite Structures*, 2007, **78**(3): 433-439.
- [5] BENATTA M A, MECHAB I, TOUNSI A, et al. Static analysis of functionally graded short beams including warping and shear deformation effects[J]. *Computational Materials Science*, 2008, **44**(2): 765-773.
- [6] ALSHORBAGY A E, ELTAHER M A, MAHMOUD F F. Free vibration characteristics of a functionally graded beam by finite element method[J]. *Applied Mathematical Modelling*, 2011, **35**(1): 412-425.
- [7] ŞİMŞEK M. Bi-directional functionally graded materials (BDFGMs) for free and forced vibration of Timoshenko beams with various boundary conditions[J]. *Composite Structures*, 2015, **133**: 968-978.
- [8] ŞİMŞEK M. Buckling of Timoshenko beams composed of two-dimensional functionally graded material (2D-FGM) having different boundary conditions[J]. *Composite Structures*, 2016, **149**: 304-314.
- [9] 滕兆春, 衡亚洲, 张会凯, 等. 弹性地基上转动 FGM 梁自由振动的 DTM 分析[J]. 计算力学学报, 2017, **34**(6): 712-717. (TENG Zhaochun, HENG Yazhou, ZHANG Huikai, et al. DTM analysis for free vibration of rotating FGM beams resting on elastic foundations[J]. *Chinese Journal of Computational Mechanics*, 2017, **34**(6): 712-717. (in Chinese))
- [10] 蒲育, 周凤玺. FGM 梁临界屈曲载荷的改进型 GDQ 法分析[J]. 应用基础与工程科学学报, 2019, **27**(6): 1308-1320. (PU Yu, ZHOU Fengxi. Critical buckling loads analysis of FGM beams by a modified generalized differential quadrature method[J]. *Journal of Basic Science and Engineering*, 2019, **27**(6): 1308-1320. (in Chinese))
- [11] WITVROUW A, MEHTA A. The use of functionally graded poly-sige layers for MEMS applications[J]. *Materials Science Forum*, 2005, **520**(492/493): 255-260.
- [12] FLECK N A, MULLER G M, ASHBY M F, et al. Strain gradient plasticity: theory and experiment[J]. *Acta Metallurgica et Materialia*, 1994, **42**(2): 475-487.
- [13] BAŽANT Z P. Size effect in blunt fracture: concrete, rock, metal[J]. *Journal of Engineering Mechanics*, 1984, **110**(4): 518-535.
- [14] YANG F, CHONG A C M, LAM D C C, et al. Couple stress based strain gradient theory for elasticity[J]. *International Journal of Solids and Structures*, 2002, **39**(10): 2731-2743.
- [15] 周强. 考虑表面效应的压电纳米梁的振动研究[J]. 应用数学和力学, 2020, **41**(8): 853-865. (ZHOU Qiang. Vibration of piezoelectric nanobeams with surface effects[J]. *Applied Mathematics and Mechanics*, 2020, **41**(8): 853-865. (in Chinese))
- [16] ŞİMŞEK M, KOCATÜRK T, AKBAŞ Ş D. Static bending of a functionally graded microscale Timoshenko beam based on the modified couple stress theory[J]. *Composite Structures*, 2013, **95**: 740-747.
- [17] KE L L, WANG Y S. Size effect on dynamic stability of functionally graded microbeams based on a modified couple stress theory[J]. *Composite Structures*, 2011, **93**(2): 342-350.
- [18] ŞİMŞEK M, REDDY J N. Bending and vibration of functionally graded microbeams using a new higher order beam theory and the modified couple stress theory[J]. *International Journal of Engineering Science*, 2013, **64**: 37-53.
- [19] AL-BASYOUNI K S, TOUNSI A, MAHMOUD S R. Size dependent bending and vibration analysis of functional-

- ly graded micro beams based on modified couple stress theory and neutral surface position[J]. *Composite Structures*, 2015, **125**: 621-630.
- [20] AKGÖZ B, CIVALEK Ö. Free vibration analysis of axially functionally graded tapered Bernoulli-Euler microbeams based on the modified couple stress theory[J]. *Composite Structures*, 2013, **98**: 314-322.
- [21] 刘松正, 张波, 沈火明, 等. 准三维功能梯度微梁的尺度效应模型及微分求积有限元[J]. *应用数学和力学*, 2021, **42**(6): 623-636.(LIU Songzheng, ZHANG Bo, SHEN Huoming, et al. A size-dependent quasi-3D functionally graded microbeam model and related differential quadrature finite elements[J]. *Applied Mathematics and Mechanics*, 2021, **42**(6): 623-636.(in Chinese))
- [22] 雷剑, 谢宇阳, 姚明格, 等. 变截面二维功能梯度微梁的振动和屈曲特性[J]. *应用数学和力学*, 2022, **43**(10): 1133-1145.(LEI Jian, XIE Yuyang, YAO Mingge, et al. Vibration and buckling characteristics of two-dimensional functionally graded microbeams with variable cross sections[J]. *Applied Mathematics and Mechanics*, 2022, **43**(10): 1133-1145.(in Chinese))
- [23] CHEN X, LU Y, LI Y. Free vibration, buckling and dynamic stability of bi-directional FG microbeam with a variable length scale parameter embedded in elastic medium[J]. *Applied Mathematical Modelling*, 2019, **67**: 430-448.
- [24] CHEN D, YANG J, KITIPORNCHAI S. Elastic buckling and static bending of shear deformable functionally graded porous beam[J]. *Composite Structures*, 2015, **133**: 54-61.
- [25] CHEN D, YANG J, KITIPORNCHAI S. Free and forced vibrations of shear deformable functionally graded porous beams[J]. *International Journal of Mechanical Sciences*, 2016, **108/109**: 14-22.
- [26] LEI Y L, GAO K, WANG X, et al. Dynamic behaviors of single- and multi-span functionally graded porous beams with flexible boundary constraints[J]. *Applied Mathematical Modelling*, 2020, **83**: 754-776.
- [27] 王伟斌, 杨文秀, 滕兆春. 多孔功能梯度材料 Timoshenko 梁的自由振动分析[J]. *计算力学学报*, 2021, **38**(5): 586-594.(WANG Weibin, YANG Wenxiu, TENG Zhaochun. Free vibration analysis of porous functionally graded materials Timoshenko beam[J]. *Chinese Journal of Computational Mechanics*, 2021, **38**(5): 586-594.(in Chinese))
- [28] WANG Xinwei. *Differential Quadrature and Differential Quadrature Based Element Methods*[M]. 2015.
- [29] TORNABENE F, FANTUZZI N, UBERTINI F, et al. Strong formulation finite element method based on differential quadrature; a survey[J]. *Applied Mechanics Reviews*, 2015, **67**(2): 020801.
- [30] 吴明明. 弹性地基上的功能梯度梁力学问题研究[D]. 硕士学位论文. 邯郸: 河北工程大学, 2019.(WU Mingming. Research on mechanical problems of functionally graded beams resting on the elastic foundation[D]. Master Thesis. Handan; Hebei University of Engineering, 2019.(in Chinese))
- [31] DENG H, CHENG W. Dynamic characteristics analysis of bi-directional functionally graded Timoshenko beams [J]. *Composite Structures*, 2016, **141**: 253-263.